BRAIN SIGNAL ANALYTICS FROM GRAPH SIGNAL PROCESSING PERSPECTIVE

Leah Goldsberry[†] *Weiyu Huang*[†] *Nicholas F. Wymbs*[‡] *Scott T. Grafton*[∗] *Danielle S. Bassett*[†] *Alejandro Ribeiro*[†]

[†]Department of Electrical and Systems Engineering, University of Pennsylvania
[‡]Department of Physical Medicine and Rehabilitation, Johns Hopkins University
∗Department of Psychological and Brain Sciences, University of California at Santa Barbara

ABSTRACT

This paper presents methods to analyze functional brain networks and signals from graph spectral perspectives. The notion of frequency and filters recently generalized to irregular graph domains defines brain graph frequencies associated with different levels of spatial smoothness across the brain regions. Brain network frequency also enables the decomposition of brain signals into pieces corresponding to smooth or rapid variations. The methods are utilized to analyze brain networks and signals as subjects master a simple motor skill. We observe that brain signals corresponding to different graph frequencies exhibit different levels of contribution to active learning. Specifically, we notice a strong association between graph spectral properties of brain networks and the level of exposure to tasks performed, and recognize the most contributing and important frequency signatures at different task familiarity.

***Index Terms*—** Functional brain network, network theory, graph signal processing, fMRI, motor learning, filtering.

1. INTRODUCTION

The study of brain activity patterns has proven valuable in identifying neurological disease and individual behavioral traits [2, 3]. The use of functional brain networks describing the tendency of different regions to act in unison has proven complementary in the analysis of similar matters [4–7]. It is not surprising that signals and networks prove useful in similar problems since the two are closely related. In this paper we advocate an intermediate path in which we interpret brain activity as a signal supported on the graph of brain connectivity. We show how the use of graph signal processing tools can be used to glean information from brain signals using the network as an aid to identify patterns of interest. The benefits of incorporating network information into signal analysis has been demonstrated in multiple domains [8–12].

The fundamental GSP concepts that we utilize to exploit brain connectivity in the analysis of brain signals are the graph Fourier transform (GFT) and the corresponding notions of graph frequency components and graph filters. These concepts are generalizations of the Fourier transform, frequency components, and filters that are used in regular domains such as time and spatial grids [13, 14]. As such, they permit the decomposition of a graph signal into components that represent different modes of variability. We can define low graph frequency components representing signals that change slowly with respect to brain connectivity networks in a well defined sense and high graph frequency components representing signals that change fast in the same sense. This is important because low and high *temporal* variability have proven important in the analysis of neurological disease and behavior [15, 16]. GFT based decompositions permit a similar analysis of variability across regions of the brain for a fixed time – a sort of *spatial* variability measured with respect to the connectivity pattern.

The goal of this paper is to introduce GSP notions that can be used to analyze brain signals and to demonstrate their value in identifying patterns that appear when monitoring activity as subjects learn to perform a visual-motor task. We begin the paper with the introduction of basic notions of graphs and graph signals (Section 2). We then move on to describe two different experiments involving the learning of different visual-motor tasks by different sets of participants (Section 3). We visualize the decomposed graph signals (Section 4) and find that high graph frequencies of functional networks concentrate on visual and sensorimotor modules of the brain – the two brain areas well-known to be associated with motor learning [17, 18]. Finally, we examine the importance of brain frequencies at different task familiarity by evaluating their respective correlation with learning performance at different task familiarities (Section 5). We find as learning progresses, we favor different levels of graph frequency components.

2. GRAPH SIGNAL PROCESSING

The interest of this paper is to study brain signals in which we are given a collection of measurements x_i associated with each cortical region out of n different brain regions. An example signal of this type is an fMRI reading in which x_i estimates the level of activity of brain region i. The collection of n measurements is henceforth grouped in the vector signal $\mathbf{x}$. A fundamental feature of the signal $\mathbf{x}$ is the existence of an underlying pattern of structural or functional connectivity that couples the values of the signal $\mathbf{x}$ at different brain regions.

We do so by modeling connectivity between brain regions with a network that is connected, weighted, and symmetric. Formally, we define a network as the pair $\mathcal{G} = (\mathcal{V}, \mathbf{W})$, where $\mathcal{V} = \{1, \ldots, n\}$ is a set of n vertices or nodes representing individual brain regions and $\mathbf{W} \in \mathbb{R}^{n \times n}$ represents weights of edges in the network with $w_{ij} \geq 0$ being the weight of the edge (i, j), in which $i, j \in \mathcal{V}$. Since the network is undirected and symmetric we have that $w_{ij} = w_{ji}$ for all (i, j). The weights $w_{ij} = w_{ji}$ represent the strength of the connection between regions i and j, or, equivalently, the proximity or similarity between nodes i and j. We adopt the conventional definitions of the degree and Laplacian matrices [19, Chapter 1]. The degree matrix $\mathbf{D} \in \mathbb{R}_{+}^{n \times n}$ is a diagonal matrix with its ith diagonal element $D_{ii} = \sum_{j=1}^{n} w_{ij}$. The Laplacian matrix is defined as the difference $\mathbf{L} := \mathbf{D} - \mathbf{W} \in \mathbb{R}^{n \times n}$. We note that brain networks, irrespective of whether their connectivity is functional [20] or structural [21], tend to be stable for a window of time, entailing associations between brain regions during captured time of interest. Brain activities can vary more frequently, forming multiple samples of brain signals supported on a common underlying network.

The graph Laplacian $\mathbf{L}$ can be decomposed into its eigenvalue components, $\mathbf{L} = \mathbf{V}\mathbf{\Lambda}\mathbf{V}^H$ such that for the set of eigenvalues $\{\lambda_k\}_{k=0,1,\ldots,n-1}$, the diagonal eigenvalue matrix is defined as $\mathbf{\Lambda} := \text{diag}(\lambda_0, \ldots, \lambda_{n-1})$, and $\mathbf{V} := [\mathbf{v}_0, \ldots, \mathbf{v}_{n-1}]$ is the eigenvector matrix. $\mathbf{V}^H$ represents

Supported by NSF CCF-1217963, PHS NS44393, ARO ICB W911NF-09-0001, ARL W911NF-10-2-0022, ARO W911NF-14-1-0679, NIH R01-HD086888, NSF BCS-1441502, NSF BCS-1430087 and the John D. and Catherine T. MacArthur and Alfred P. Sloan foundations. A journal version of the paper can be found in [1].

the Hermitian (conjugate transpose) of the matrix $\mathbf{V}$. We assume the eigenvalues of the Laplacian $\mathbf{L}$ are ordered so that $0 = \lambda_0 \leq \lambda_1 \leq \ldots \leq \lambda_{n-1}$. The eigenvector matrix $\mathbf{V}$ is used to define the Graph Fourier Transform of the graph signal $\mathbf{x}$ as we next [14].

Definition 1 *Given a signal $\mathbf{x} \in \mathbb{R}^n$ and a graph Laplacian $\mathbf{L} \in \mathbb{R}^{n \times n}$, the Graph Fourier Transform (GFT) of $\mathbf{x}$ with respect to $\mathbf{L}$ is the signal $\tilde{\mathbf{x}} := \mathbf{V}^H \mathbf{x}$. The inverse (i)GFT of $\tilde{\mathbf{x}}$ with respect to $\mathbf{L}$ is defined as $\mathbf{x} := \mathbf{V}\tilde{\mathbf{x}}$. We say that $\mathbf{x}$ and $\tilde{\mathbf{x}}$ form a GFT pair.*

An important property of the GFT is that it encodes a notion of variability akin to the notion of variability that the Fourier transform encodes for temporal signals. Given a graph signal $\mathbf{x}$ with GFT $\tilde{\mathbf{x}}$ we can isolate the frequency components corresponding to the lowest K_{L} graph frequencies by defining the filtered spectrum $\tilde{\mathbf{x}}_{\text{L}} := \tilde{\mathbf{H}}_{\text{L}} \tilde{\mathbf{x}}$ satisfying $\tilde{x}_{\text{L}k} = \tilde{x}_k$ for $k < K_L$ and $\tilde{x}_{\text{L}k} = 0$ otherwise. The filter $\tilde{\mathbf{H}}_{\text{L}}$ can be written as the diagonal matrix $\tilde{\mathbf{H}}_{\text{L}} := \text{diag}(\tilde{\mathbf{h}}_{\text{L}})$ where the vector $\tilde{\mathbf{h}}_{\text{L}}$ takes value 1 for frequencies smaller than K_{L} and is otherwise null, $\tilde{h}_{\text{L}k} = \mathbb{I}\big[k < K_{\text{L}}\big]$. Utilizing the definitions of the GFT and the iGFT, the spectral operation $\tilde{\mathbf{x}}_{\text{L}} = \tilde{\mathbf{H}}_{\text{L}} \tilde{\mathbf{x}}$ is equivalent to performing the following operations in the graph vertex domain $\mathbf{x}_{\text{L}} = \mathbf{V}\tilde{\mathbf{x}}_{\text{L}} = \mathbf{V}\tilde{\mathbf{H}}_{\text{L}}\tilde{\mathbf{x}} = \mathbf{V}\tilde{\mathbf{H}}_{\text{L}}\mathbf{V}^{-1}\mathbf{x} =: \mathbf{H}_{\text{L}}\mathbf{x}$. From this equality, we can see that the signal $\mathbf{x}_{\text{L}}$ contains the low graph frequency components of $\mathbf{x}$, and so we say the matrix $\mathbf{H}_{\text{L}}$ is a *graph low-pass filter*.

The filter $\mathbf{H}_{\text{L}} := \mathbf{V}\tilde{\mathbf{H}}_{\text{L}}\mathbf{V}^{-1}$ admits an alternative representation as the expansion $\mathbf{H}_{\text{L}} = \sum_{k=0}^{n-1} h_{\text{L}k}\mathbf{L}^k$ in terms of Laplacian powers. Since the eigenvalues are ordered, the coefficients $h_{\text{L}k}$ tend to be concentrated in small indexes k, and the expansion $\mathbf{H}_{\text{L}} = \sum_{k=0}^{n-1} h_{\text{L}k}\mathbf{L}^k$ is therefore dominated by small powers $\mathbf{L}^k$. From this fact it follows that we can think of the graph low-pass filtered signal $\mathbf{x}_{\text{L}}$ as resulting from a localized averaging of the elements of $\mathbf{x}$. To understand this interpretation, simply note that $\mathbf{L}^0\mathbf{x} = \mathbf{x}$ coincides with the original signal, $\mathbf{L}\mathbf{x}$ is an average of neighboring elements, $\mathbf{L}^2\mathbf{x}$ is an average of elements in nodes that interact via intermediate common neighbors, and, in general, $\mathbf{L}^k\mathbf{x}$ describes interactions between k-hop neighbors. The fact that $\mathbf{x}_{\text{L}}$ can be considered as a signal that follows from local averaging of $\mathbf{x}$ implies that $\mathbf{x}_{\text{L}}$ has smaller total variation than $\mathbf{x}$.

Other types of graph filters can be defined analogously to study interactions between signal components other than the local interactions captured in $\mathbf{x}_{\text{L}}$. Apart from the graph low-pass filter $\mathbf{H}_{\text{L}}$, we also consider a graph band-pass filter $\mathbf{H}_{\text{M}}$ and a graph high-pass filter $\mathbf{H}_{\text{H}}$, whose graph frequency responses are defined as $\tilde{h}_{\text{M}k} = \mathbb{I}\big[K_{\text{L}} \leq k < K_{\text{L}} + K_{\text{M}}\big]$ and $\tilde{h}_{\text{H}k} = \mathbb{I}\big[K_{\text{L}} + K_{\text{M}} \leq k\big]$. The definitions for filters are such that the low-pass filter takes the lowest K_{L} graph frequencies, the band-pass filter captures the middle K_{M} graph frequencies, and the high-pass filter the highest $n - K_{\text{L}} - K_{\text{M}}$ frequencies. The three filters are defined such that the graph frequencies of their respective interest are mutually exclusive yet collectively exhaustive. As a result, if we use $\mathbf{x}_{\text{M}} := \mathbf{H}_{\text{M}}\mathbf{x}$ and $\mathbf{x}_{\text{H}} := \mathbf{H}_{\text{H}}\mathbf{x}$ to respectively denote the signals filtered by the band-pass and high-pass filters, we have that the original signal can be written as the sum $\mathbf{x} = \mathbf{x}_{\text{L}} + \mathbf{x}_{\text{M}} + \mathbf{x}_{\text{H}}$. This gives a decomposition of $\mathbf{x}$ into low, medium, and high frequency components which respectively represent signals that have slow, medium, and high variability with respect to the connectivity network between brain regions. This decomposition is utilized in this paper to analyze brain activity patterns associated with the learning of visual-motor tasks.

3. BRAIN SIGNALS DURING LEARNING

We considered two experiments in which subjects learned a simple motor task [22, 23]. In the experiments, fourty-seven right-handed participants (mean age 24.13 years) volunteered with informed consent in accordance with the University of California, Santa Barbara Internal Review Board. After exclusions for task accuracy, incomplete scans, and abnormal MRI, 38 participants were retained for subsequent analysis.

	Session 1	Session 2	Session 3	Session 4
MIN Sequences	50	110	170	230
MOD Sequences	50	200	350	500
EXT Sequences	50	740	1430	2120

Fig. 1. Relationship between training duration, intensity, and depth for the first experimental framework.

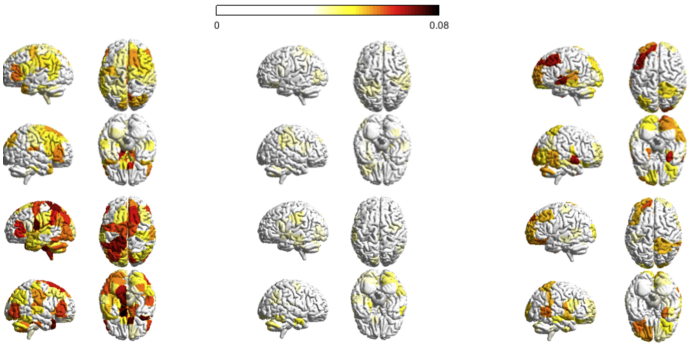

Fig. 2. Distribution of decomposed signals for the 6 week experiment (Top) and 3 day experiment (Bottom). Decomposed signal $\mathbf{x}_{\text{L}}$ averaged across all subjects is plotted on the left, $\mathbf{x}_{\text{M}}$ on the middle, and $\mathbf{x}_{\text{H}}$ on the right.

Twenty individuals participated in the first experimental framework. The experiment lasted 6 weeks, in which there were 4 scanning sessions, roughly at the start of the experiment, at the end of the 2nd week, at the end of the 4th week, and at the end of the experiment, respectively. During each scanning session, individuals performed a discrete sequence-production task in which they responded to sequentially presented stimuli with their dominant hand on a custom response box. Sequences were presented using a horizontal array of 5 square stimuli with the responses mapped from left to right such that the thumb corresponded to the leftmost stimulus. The next square in the sequence was highlighted immediately following each correct key press; the sequence was paused awaiting the depression of the appropriate key if an incorrect key was pressed. Each participant completed 6 different 10-element sequences. Each sequence consists of two squares per key. Participants performed the same sequences at home between each two adjacent scanning sessions, however, with different levels of exposure for different sequence types. Therefore, the number of trials completed by the participants after the end of each scanning session depends on the sequence type. There are 3 different sequence types (MIN, MOD, EXT) with 2 sequences per type. The number of trials of each sequence type completed after each scanning session averaged over the 20 participants is summarized in Fig. 1. Eighteen subjects participated in the second experimental framework. The experiment had 3 scanning sessions spanning the three days. Each scanning session lasted roughly 2 hours and no training was performed at home between adjacent scanning sessions. Subjects responded to a visually cued sequence by generating responses using the four fingers of their nondominant hand on a custom response box. Visual cues were presented as a series of musical notes on a pseudo-musical staff with four lines such that the top line of the staff mapped to the leftmost key pressed with the pinkie finger. Each 12-note sequence randomly ordered contained three notes per line. Each training epoch involved 40 trials and lasted a total of 245 repetition times (TRs), with a TR of 2,000 ms. Each training session contained 6 scan epochs (240 trials) and lasted a total of 2,070 scan TRs. In both experiments participants were instructed to respond promptly and accurately. Repetitions (e.g., "11") and regularities such as trills (e.g., "121") and runs (e.g., "123") were excluded in all sequences. The order and number of sequence trials were identical for all participants. Participants completed the tasks inside the MRI scanner

for scanning sessions.

Reordering with fMRI was conducted using a 3.0 T Siemens Trio with a 12-channel phased-array head coil. For each functional run, a single-shot echo planar imaging sequence that is sensitive to blood oxygen level dependent (BOLD) contrast was utilized to obtain 37 (the first experiment) or 33 (the second experiment) slices (3mm thickness) per repetition time (TR), an echo time of 30 ms, a flip angle of 90°, a field of view of 192 mm, and a 64×64 acquisition matrix. Image preprocessing was performed using the Oxford Center for Functional Magnetic Resonance Imaging of the Brain (FMRIB) Software Library (FSL), and motion correction was performed using FMRIB's linear image registration tool. The whole brain is parcellated into a set of $n = 112$ regions of interest that correspond to the 112 cortical and subcortical structures anatomically identified in FSL's Harvard-Oxford atlas. The threshold in probability cutoff settings of Harvard Oxford atlas parcellation is 0 so that no voxels were excluded.

For each individual fMRI dataset, we estimate regional mean BOLD time series by averaging voxel time series in each of the n regions. We evaluate the magnitude squared spectral coherence [24] between the activity of all possible pairs of regions to construct $n \times n$ functional connectivity matrices $\mathbf{W}$. Besides, for each pair of brain regions i and j, we use t-statistical testing to evaluate the probability $p_{i,j}$ of observing the measurements by random chance, when the actual data are uncorrelated [25]. In the 3 day dataset, the value of all elements with no statistical significance ($p_{i,j} > 0.05$) [26] are set to zero; the values remain unchanged otherwise. In the 3 day experiment, a single brain network is constructed for each participant. Thresholding is applied because the networks are for the entire span of the experiment and many entries in $\mathbf{W}$ would be close to zero without threshold correction. In the 6 week experiment, due to the long duration of the experiment, we build a different brain network per scanning session, per sequence type for each subject. Because each network describes the functional connectivity for one training session given a subject, not many entries will be removed even in the presence of threshold correction; consequently, no thresholding is applied for the 6 week dataset. We normalize the regional mean BOLD observations $\hat{\mathbf{x}}(t)$ at any sample time t and consider $\mathbf{x}(t) = \hat{\mathbf{x}}(t)/\|\hat{\mathbf{x}}(t)\|_2$ such that the total energy of activities at all structures is consistent at different t to avoid extreme spikes due to head motion or drift artifacts in fMRI.

4. FREQUENCY DECOMPOSITION OF BRAIN SIGNALS

We investigate brain signals from a GSP perspective, and analyze the brain signals by examining the decomposed graph signals $\mathbf{x}_{\mathrm{L}}, \mathbf{x}_{\mathrm{M}}$, and $\mathbf{x}_{\mathrm{H}}$ with respect to the underlying brain networks. We compute the absolute magnitude of the decomposed signal $\mathbf{x}_{\mathrm{L}}$ for each brain region averaged across all sample signals for each individual during a scan session and then averaged across all participants. Similar aggregation is applied for $\mathbf{x}_{\mathrm{M}}$ and $\mathbf{x}_{\mathrm{H}}$. Fig. 2 presents the distribution of the decomposed signals corresponding to different levels of spatial variations for in both the two experiments considered (Top: first scan session in the 6 week experiment and Bottom: 3 day experiment). Other scan sessions in 6 week experiment yield similar results. Brain regions with absolute magnitudes lower than a fixed threshold are not colored.

A deep analysis of Fig. 2 yields many interesting aspects of graph frequency decomposition. First, for $\mathbf{x}_{\mathrm{L}}$, the magnitudes on adjacent brain regions tend to possess highly similar values, resulting in a more evenly spread brain signal distribution, where as for $\mathbf{x}_{\mathrm{H}}$, neighboring signals can exhibit highly dissimilar values; this corroborates the motivation to use graph frequency decomposition to segment brain signals into pieces corresponding to different levels of spatial fluctuations. Second, decomposed signals for a specific level of variation, notedly $\mathbf{x}_{\mathrm{H}}$, are highly similar with respect to different scan sessions in an experiment as well as with respect to the two experiments with different sets of participants. The correlation coefficient between datasets for high graph frequencies is 0.6469. Third, recall that we normalize the brain signals at every sample point for all subjects, and for this reason signals $\mathbf{x}_{\mathrm{L}}, \mathbf{x}_{\mathrm{M}}$ and $\mathbf{x}_{\mathrm{H}}$ would be similarly distributed across the brain if nothing interesting happens at the decomposition. However, in both Fig. 2, it is observed that many brain regions possess magnitudes higher than a threshold in $\mathbf{x}_{\mathrm{L}}$ ($\sim 60\%$ pass) and $\mathbf{x}_{\mathrm{H}}$ ($\sim 20\%$ pass) while not many brain regions pass the thresholding with respect to $\mathbf{x}_{\mathrm{M}}$ ($\sim 3\%$ pass). It has long been understood that the brain combines some degree of disorganized behavior with some degree of regularity and that the complexity of a system is high when order and disorder coexist [27]. $\mathbf{x}_{\mathrm{L}}$ varies smoothly across the brain network and therefore can be regarded as regularity (order), whereas $\mathbf{x}_{\mathrm{H}}$ fluctuates rapidly and consequently can be considered as randomness (disorder). This evokes the intuition that graph frequency decomposition segments a brain signal $\mathbf{x}$ into pieces $\mathbf{x}_{\mathrm{L}}$ and $\mathbf{x}_{\mathrm{H}}$, which reflect order and disorder (and are therefore more interesting), as well as the remaining $\mathbf{x}_{\mathrm{M}}$.

	$\|\mathbf{x}_{\mathrm{L}}\|_2$	$\|\mathbf{x}_{\mathrm{M}}\|_2$	$\|\mathbf{x}_{\mathrm{H}}\|_2$
6 week experiment (linear scale)	-0.3155	0.0897	0.4125
6 week experiment (logarithm scale)	-0.5409	0.3992	0.3565
3 day experiment	-0.9873	0.8443	0.9605

Fig. 3. Pearson correlation coefficients between the number of trials (level of task familiarity) and R values, defined as correlations between learning rate parameters and the norm of the decomposed signal of interest. Decreasing association with exposure to tasks is observed for the $\|\mathbf{x}_{\mathrm{L}}\|_2$ and increasing importance is noticed for $\|\mathbf{x}_{\mathrm{H}}\|_2$.

5. FREQUENCY SIGNATURES OF TASK FAMILIARITIES

Given a participant, for each sequence completed, we defined the movement time M as the difference between the time of the first button press and the time of the last button press during a single sequence. We then estimate the participant's learning rate by fitting an exponential function (plus a constant) using the robust outlier correction [28] to the sequence of movement times $\mathbf{M}$,

$$\mathbf{M} = c_1 e^{\mathbf{t}/\kappa} + c_2. \tag{1}$$

where $\mathbf{t}$ is a sequence representing the time index, κ is the exponential drop-off parameter (which we call the "learning rate parameter") used to describe the early and fast rate of improvement, and c_1 and c_2 are nonnegative constants. A negative value of κ indicates a decrease in movement time $M(t)$, which is thought to indicate that learning is occurring [29]. We chose exponential because it is viewed as the most statistically robust choice [30]. Further, the approach that we used has the advantage of estimating the rate of learning independent of initial performance or performance ceiling.

We evaluate the learning rate for all participants at each scanning session, and then compute the correlation between the norm $\|\mathbf{x}_{\mathrm{L}}\|_2$ of the decomposed signal corresponding to low spatial variation and the learning rates across subjects. The correlation (R value) between the norms $\|\mathbf{x}_{\mathrm{M}}\|_2$ as well as $\|\mathbf{x}_{\mathrm{H}}\|_2$ and learning rates are also calculated. Fig. 4 plots the Pearson correlation coefficients at all scanning sessions of the two experiments considered. The horizontal axis denotes the level of exposure of participants to the sequence – which day in the 3 day experiment and how many number of trials participants have completed at the end of the scanning session in the 6 week experiment. Points are densely distributed for small number of trials in the 6 week experiment, so to mitigate this effect, we also plot the points by taking the logarithm of numbers of trials completed. We emphasize that due to normalization at each sampling point, the correlation values would all be 0 if graph frequency decomposition segments brain signals into three equivalent pieces. There are scan sessions where the correlation is of particular

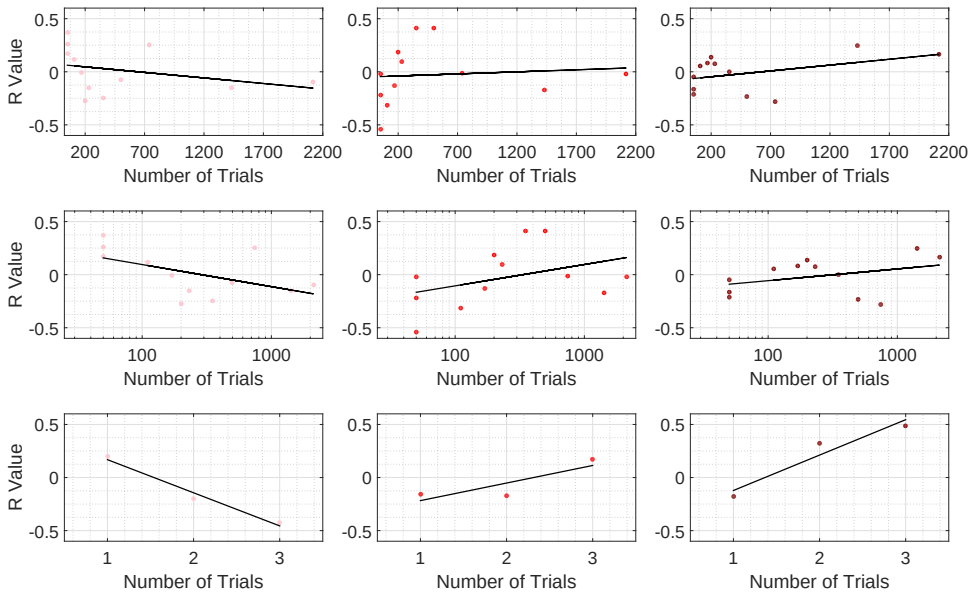

Fig. 4. Scatter plots in which each point is for a specific training session (level of task familiarity), depicting the R value defined here as correlations between learning rate parameters and the norm of the decomposed signal of interest (Left: $\mathbf{x}_{\mathrm{L}}$, Middle: $\mathbf{x}_{\mathrm{M}}$, and Right: $\mathbf{x}_{\mathrm{H}}$). Top: 6 week experiment with number of trials in linear scale. Middle: 6 week experiment logarithm scale. Bottom row: 3 day experiment.

interest, however the most noteworthy observation is the change of correlation values with the level of exposure for participants.

In general, for $\mathbf{x}_{\mathrm{L}}$ corresponding to smooth spatial variation, we see a gradually decreasing trend in correlation with learning as training progresses. Although not all training sessions can be fit to this pattern (i.e. trials 500 and 740), it is still visible that the correlation with learning is above zero (≈ 0.25) at the start of the training when participants perform the task for the first time and gradually shifts to below zero (≈ -0.25) at the end of the experiment when individuals are highly familiar with the sequence. For $\mathbf{x}_{\mathrm{H}}$ corresponding to vibrant spatial variation, its correlation with learning is below zero (≈ -0.2) at the start of the training, and gradually increases throughout training until it is above zero (≈ 0.25) at the end of the experiment, with the exception of trials 500 and 740. This is the exact opposite of $\mathbf{x}_{\mathrm{L}}$. For $\mathbf{x}_{\mathrm{M}}$, correlation between its norm $\|\mathbf{x}_{\mathrm{M}}\|_2$ with learning rate generally increases with the intensity of training. However, this trend is not as obvious compared to other decomposition counterparts, and there are a greater number of sessions that cannot be fit to this pattern. The correlation between the number of trials and R values is summarized in Fig. 3. The results presented are robust with similar values in filter thresholds.

This result further implies that the most association between learning or adaptability during the training process comes from the brain signals that either vary smoothly ($\mathbf{x}_{\mathrm{L}}$, regularity) or rapidly ($\mathbf{x}_{\mathrm{H}}$, randomness) with respect to the brain network. Therefore, the graph frequency decomposition could be used to capture more informative brain signals by filtering out non-informative counterparts, most likely associated with middle graph frequencies. Besides, the positive association between $\|\mathbf{x}_{\mathrm{L}}\|_2$ and learning rates as well as the negative association between $\|\mathbf{x}_{\mathrm{H}}\|_2$ and learning rates at the start of training indicates that it favors learning to have more *smooth*, *spread*, and *cooperative* brain signals when we face an unfamiliar task. As we gradually become familiar with the task, the smooth and cooperative signal distribution becomes less and less important, and there is a level of exposure when such signal distribution becomes destructive instead of constructive. We note that the task in the 3 day experiment is more difficult compared to that of the 6 week experiment, and therefore the time when the cooperative signal distribution starts to become detrimental (the point where the regression line intercepts the horizontal line of R value equaling 0) is also comparable in the two experiments, describing a certain level of familiarity to the task. When we become highly familiar with the task, it favors further learning to have *varied*, *spiking*, and *competitive* brain signals.

In the dataset evaluated here, we utilize the average coherence between time series at pairs of brain cortical and subcortical regions during the training as the network. Hence, a concentration of brain activities towards low graph frequencies would imply that activities on brain regions that are generally cooperative are indeed similar. Simultaneously, the interpretation of concentration of brain activities towards high graph frequencies is that brain activities on brain regions that are generally cooperative are in fact dissimilar. In terms of learning, one possible explanation is that there are two different stages in learning: we start by grasping the big picture of the task to perform relatively well, and then we refine the details to perform better and to approach our limits.

Because the graph frequency analysis method presented in this paper applies to any setting where signals are defined on top of a network structure representing proximities between nodes, it would be interesting in future to use this method to investigate other types of signals and networks in neuroscience problems. As an example, in situations given fMRI measurements on structural networks, concentration of signals in low graph frequency components would imply functional activities do behave according to the structural networks. Besides, it has been understood that learning is different when one is unfamiliar or familiar with a particular task – it is easy to improve performance at first exposure due to the fact that one is far from their performance ceiling. It would therefore be interesting to utilize graph frequency decomposition to further analyze the difference between learning scenarios at different stages of familiarity, e.g. adaptability at first exposure and creativity when one fully understands the components of the specific tasks.

6. CONCLUSION

We used graph spectrum methods to analyze functional brain networks and signals during simple motor learning tasks. We discerned that brain activities corresponding to different graph frequencies. Further, the strong correlation between graph spectrum of brain networks with the level of familiarity of tasks was observed, and the most contributing frequency signatures at different task familiarity was recognized.

7. REFERENCES

[1] W. Huang, L. Goldsberry, N. F. Wymbs, S. T. Grafton, D. S. Bassett, and A. Ribeiro, "Graph frequency analysis of brain signals," *J. Sel. Topics Signal Process.*, vol. 10, no. 7, pp. 1189–1203, October 2016.

[2] H. Haken, *Principles of Brain Functioning: a Synergetic Approach to Brain Activity, Behavior and Cognition*. Springer Science & Business Media, 2013, vol. 67.

[3] M. D. Fox and M. E. Raichle, "Spontaneous fluctuations in brain activity observed with functional magnetic resonance imaging," *Nature Reviews Neuroscience*, vol. 8, no. 9, pp. 700–711, 2007.

[4] J. D. Medaglia, W. Huang, E. A. Karuza, S. L. Thompson-Schill, A. Ribeiro, and D. S. Bassett, "Functional alignment with anatomical networks is associated with cognitive flexibility," *Nature Human Behavior*, vol. (submitted.), November 2016. [Online]. Available: https://arxiv.org/pdf/1611.08751v1.pdf

[5] J. D. Medaglia, W. Huang, S. Segarra, C. Olm, J. Gee, M. Grossman, A. Ribeiro, C. T. McMillan, and D. S. Bassett, "Brain network efficiency is influenced by pathological source of corticobasal syndrome," *Neurology*, vol. (revised), October 2016. [Online]. Available: https://arxiv.org/pdf/1601.07867v1.pdf

[6] S. Achard, R. Salvador, B. Whitcher, J. Suckling, and E. Bullmore, "A resilient, low-frequency, small-world human brain functional network with highly connected association cortical hubs," *The Journal of neuroscience*, vol. 26, no. 1, pp. 63–72, 2006.

[7] E. Bullmore and O. Sporns, "The economy of brain network organization," *Nature Reviews Neuroscience*, vol. 13, no. 5, pp. 336–349, 2012.

[8] H. Q. Nguyen, P. Chou, Y. Chen *et al.*, "Compression of human body sequences using graph wavelet filter banks," in *Acoustics, Speech and Signal Processing (ICASSP), 2014 IEEE International Conference on*. IEEE, 2014, pp. 6152–6156.

[9] S. Segarra, W. Huang, and A. Ribeiro, "Diffusion and superposition distances for signals supported on networks," *IEEE Trans Signal Inform Process Networks*, vol. 1, no. 1, pp. 20–32, March 2015.

[10] J. Ma, W. Huang, S. Segarra, and A. Ribeiro, "Diffusion filtering for graph signals and its use in recommendation systems," in *Proc. Int. Conf. Acoustics Speech Signal Process*, Shanghai, China, 2016, pp. 4563 – 4567.

[11] A. Gadde, A. Anis, and A. Ortega, "Active semi-supervised learning using sampling theory for graph signals," in *Proceedings of the 20th ACM SIGKDD international conference on Knowledge discovery and data mining*. ACM, 2014, pp. 492–501.

[12] W. Huang, A. G. Marques, and A. Ribeiro, "Collaborative filtering and matrix completion via graph filtering," in *European Signal Process. Conf. (EUSIPCO)*, Kos Island, Greece, August 28 - September 2 2017, p. (invited).

[13] A. Sandryhaila and J. M. Moura, "Discrete signal processing on graphs," *IEEE Trans Signal Process*, vol. 61, no. 7, pp. 1644–1656, 2013.

[14] D. Shuman, S. K. Narang, P. Frossard, A. Ortega, P. Vandergheynst *et al.*, "The emerging field of signal processing on graphs: Extending high-dimensional data analysis to networks and other irregular domains," *IEEE Signal Process Mag*, vol. 30, no. 3, pp. 83–98, 2013.

[15] D. D. Garrett, N. Kovacevic, A. R. McIntosh, and C. L. Grady, "The modulation of bold variability between cognitive states varies by age and processing speed," *Cerebral Cortex*, p. bhs055, 2012.

[16] J. J. Heisz, J. M. Shedden, and A. R. McIntosh, "Relating brain signal variability to knowledge representation," *Neuroimage*, vol. 63, no. 3, pp. 1384–1392, 2012.

[17] J. A. Kleim, S. Barbay, N. R. Cooper, T. M. Hogg, C. N. Reidel, M. S. Remple, and R. J. Nudo, "Motor learning-dependent synaptogenesis is localized to functionally reorganized motor cortex," *Neurobiology of learning and memory*, vol. 77, no. 1, pp. 63–77, 2002.

[18] D. S. Bassett, M. Yang, N. F. Wymbs, and S. T. Grafton, "Learning-induced autonomy of sensorimotor systems," *Nature neuroscience*, vol. 18, no. 5, pp. 744–751, 2015.

[19] F. Chung, *Spectral graph theory*. American Mathematical Soc., 1997, vol. 92.

[20] W.-T. Zhang, Z. Jin, G.-H. Cui, K.-L. Zhang, L. Zhang, Y.-W. Zeng, F. Luo, A. C. Chen, and J.-S. Han, "Relations between brain network activation and analgesic effect induced by low vs. high frequency electrical acupoint stimulation in different subjects: a functional magnetic resonance imaging study," *Brain research*, vol. 982, no. 2, pp. 168–178, 2003.

[21] J. Grutzendler, N. Kasthuri, and W.-B. Gan, "Long-term dendritic spine stability in the adult cortex," *Nature*, vol. 420, no. 6917, pp. 812–816, 2002.

[22] D. S. Bassett, N. F. Wymbs, M. P. Rombach, M. A. Porter, P. J. Mucha, and S. T. Grafton, "Task-based core-periphery organization of human brain dynamics," *PLoS Comput. Biol*, vol. 9, no. 9, p. e1003171, 2013.

[23] N. F. Wymbs, D. S. Bassett, P. J. Mucha, M. A. Porter, and S. T. Grafton, "Differential recruitment of the sensorimotor putamen and frontoparietal cortex during motor chunking in humans," *Neuron*, vol. 74, no. 5, pp. 936–946, 2012.

[24] F. T. Sun, L. M. Miller, and M. D'Esposito, "Measuring interregional functional connectivity using coherence and partial coherence analyses of fmri data," *Neuroimage*, vol. 21, no. 2, pp. 647–658, 2004.

[25] Y. He, Z. J. Chen, and A. C. Evans, "Small-world anatomical networks in the human brain revealed by cortical thickness from mri," *Cereb cortex*, vol. 17, no. 10, pp. 2407–2419, 2007.

[26] C. R. Genovese, N. A. Lazar, and T. Nichols, "Thresholding of statistical maps in functional neuroimaging using the false discovery rate," *Neuroimage*, vol. 15, no. 4, pp. 870 – 878, 2002.

[27] O. Sporns, *Networks of the Brain*. MIT press, 2011.

[28] D. A. Rosenbaum, *Human motor control*. Academic press, 2009.

[29] E. Dayan and L. G. Cohen, "Neuroplasticity subserving motor skill learning," *Neuron*, vol. 72, no. 3, pp. 443–454, 2011.

[30] A. Heathcote, S. Brown, and D. Mewhort, "The power law repealed: The case for an exponential law of practice," *Psychonomic bulletin & review*, vol. 7, no. 2, pp. 185–207, 2000.